International Journal of Heat and Mass Transfer 52 (2009) 4966–4975

Contents lists available at ScienceDirect

International Journal of Heat and Mass Transfer

journal homepage: www.elsevier.com/locate/ijhmt

Heat transfer through coupled thermal boundary layers induced by a suddenly generated temperature difference

Feng Xu *, John C. Patterson, Chengwang Lei

School of Engineering, James Cook University, Townsville, Qld 4811, Australia

ARTICLE INFO

Article history:
Received 29 May 2008
Received in revised form 28 October 2008
Available online 3 July 2009

Keywords:
Coupled thermal boundary layers
Transient natural convection
Differentially heated partitioned cavity

ABSTRACT

The coupled thermal boundary layers adjacent to a partition in a differentially heated cavity are numerically investigated. The cavity is filled with water, which is initially quiescent but with an imposed temperature difference between the two sides of the vertical partition. The numerical results show that the development of natural convection flows in the partitioned cavity undergoes three main stages: an initial stage, a transitional stage and a steady stage. The transient features of the coupled thermal boundary layers adjacent to the partition as well as the overall natural convection flow in the partitioned cavity are described, and heat transfer through the coupled thermal boundary layers and the partitioned cavity is examined.

1. Introduction

It is expected that when a fluid container is suddenly placed in an ambient fluid of a different temperature, fluid motions will occur on both sides of the vertical wall of the container due to heat transfer through the wall. This is relevant to many situations in nature and engineering, one example of which is an oil tank of a wrecked ship submerged in the sea [1]. In previous studies, the presence of a thermal boundary layer outside the vertical wall of the container is often ignored, and a typical scenario is that the vertical wall is considered isothermal (see e.g. [1]). However, it is clear that thermal boundary layers are present on both sides of the vertical wall in real situations, and the coupling between these thermal boundary layers may significantly impact on heat transfer through the vertical wall. This has motivated the present investigation, which is concerned with heat transfer across such a partition in a differentially heated cavity, taking into account the coupling effect of dual boundary layers, as well as the overall natural convection flow in the partitioned cavity. This study is therefore of fundamental interest and of practical significance.

Indeed, natural convection in a differentially heated cavity has received considerable attention in the literature. Previous studies (e.g. [2]) showed that for low Rayleigh numbers (e.g. $<10^3$), conduction dominates heat transfer through the cavity. However, for higher Rayleigh numbers, convective heat transfer becomes dominant, and distinct thermal boundary layers adjacent to the cooled and heated sidewalls are formed and the fluid in the core becomes stratified at the steady state (see e.g. [3–6]). As the Rayleigh number increases further and becomes larger than a certain critical value, the flow becomes time-periodic, characterized by internal gravity waves in the core and travelling waves in the thermal boundary layer (e.g. [7–12]). If the Rayleigh number is sufficiently large, natural convection in the cavity may eventually become turbulent (e.g. [13–15]).

The majority of the early work on this topic has focused on fully developed flows. However, due to the extensive presence of transient forcing in nature and in industry, transient natural convection in the differentially heated cavity following sudden heating and cooling has been paid increasing attention over the past three decades. Fundamental scaling relations quantifying transient natural convection, including the development of the thermal boundary layers adjacent to the sidewalls and the horizontal intrusion flows along the horizontal walls were obtained by Patterson and Imberger [8]. Subsequently, other transient features of natural convection in the cavity such as the leading edge effect (LEE) in the thermal boundary layers at an initial stage and trailing waves in the horizontal intrusion at the transitional stage were investigated (e.g. [16–20]).

In addition to the above-mentioned studies of a basic model of differentially heated cavities, the study of natural convection in a differentially heated cavity with an interior conducting vertical partition has also been given considerable attention due to its relevance to industrial applications (e.g. [21]). In this case, the heat transfer between the two differentially heated sidewalls is controlled by the heat transfer across the partition, and an understanding of the mechanisms which control that transfer is essential for optimizing or otherwise controlling the overall heat transfer.

* Corresponding author. Tel.: +61 7 4781 4420; fax: +61 7 4781 6788.
E-mail address: feng.xu@jcu.edu.au (F. Xu).

0017-9310/$ - see front matter © 2009 Elsevier Ltd. All rights reserved.
doi:10.1016/j.ijheatmasstransfer.2009.06.004

Nomenclature

A	aspect ratio
g	acceleration due to gravity
H, L	height and length of the cavity
N	number of the partitions
Nu_y, Nu	local and overall Nusselt number
Pr	Prandtl number
p, $p*$	dimensionless and dimensional pressure
Ra	Rayleigh number
Q	volumetric flow rate
S	stratification parameter ($\partial T/\partial y$)
T, $T*$	dimensionless and dimensional temperature
T_0	initial average temperature of the fluid in the cavity
T_c, T_h	temperatures of the cold and hot sidewalls
T_i, T_P	initial temperatures of the interior fluid and the partition (or sidewall)
ΔT	temperature difference between the hot and cold sidewalls
t, $t*$	dimensionless and dimensional time
t_s	time for convection to balance conduction
t_f	time for the cavity to be filled up with the thermal fluid discharged from the coupled thermal boundary layers
Δt	time step
u, v	dimensionless velocities in x- and y-directions
$u*$, $v*$	dimensional velocities in x- and y-directions
x, y	dimensionless horizontal and vertical coordinates
$x*$, $y*$	dimensional horizontal and vertical coordinates
β	coefficient of thermal expansion
δ_T	thickness of the thermal boundary layer
κ	thermal diffusivity
ν	kinematic viscosity

For a laminar flow regime, previous studies have shown that such a partition, even though perfectly conducting, depresses natural convection in the cavity in comparison with that in a non-partitioned cavity, and thus heat transfer through the cavity is significantly reduced (e.g. [21–23]). The relationship between heat transfer and the Rayleigh number, quantified by the Nusselt number scale $Nu \sim Ra^{1/4}$, has been confirmed by, for example, Anderson and Bejan [24,25]. Since the partition depresses heat transfer through the cavity, a further attempt to place additional partitions into the cavity to further depress or suppress natural convection has practical significance. Experimental and numerical results (e.g. [26]) show that the Nusselt number on the sidewall is inversely proportional to $(1 + N)$, where N is the number of partitions.

All of these studies of natural convection in a partitioned cavity have been in the context of steady flows. However, inspired by the above-mentioned transient flow phenomena (e.g. the cooling process of an oil tank of a wrecked ship immersed in the sea [1]), this study considers transient natural convection resulting from a suddenly generated temperature difference between the fluids on the two sides of a conducting partition. A phenomenon of particular interest in the transient flow development is that the temperature condition on the partition changes from initially isothermal to approximately isoflux at the steady state. The impact of the partition on transient heat transfer is also discussed.

In the remainder of this paper, the numerical procedures are described in Section 2. Transient features of natural convection in a partitioned cavity following a suddenly generated temperature difference between the fluids on the two sides of the partition are characterized in Section 3. Heat transfer through the partitioned cavity is discussed in Sections 4 and 5 summarizes the major conclusions drawn from the study.

2. Numerical procedures

Under consideration is a two-dimensional partitioned cavity (height H and width L), which is illustrated in Fig. 1. The development of natural convection in the partitioned cavity is governed by the following dimensionless two-dimensional Navier–Stokes and energy equation with the Boussinesq approximation:

$$\frac{\partial u}{\partial x}+\frac{\partial v}{\partial y}=0, \tag{1}$$

$$\frac{\partial u}{\partial t}+u\frac{\partial u}{\partial x}+v\frac{\partial u}{\partial y}=-\frac{\partial p}{\partial x}+\frac{Pr}{Ra^{1/2}}\left(\frac{\partial^2 u}{\partial x^2}+\frac{\partial^2 u}{\partial y^2}\right), \tag{2}$$

$$\frac{\partial v}{\partial t}+u\frac{\partial v}{\partial x}+v\frac{\partial v}{\partial y}=-\frac{\partial p}{\partial y}+\frac{Pr}{Ra^{1/2}}\left(\frac{\partial^2 v}{\partial x^2}+\frac{\partial^2 v}{\partial y^2}\right)+PrT, \tag{3}$$

$$\frac{\partial T}{\partial t}+u\frac{\partial T}{\partial x}+v\frac{\partial T}{\partial y}=\frac{1}{Ra^{1/2}}\left(\frac{\partial^2 T}{\partial x^2}+\frac{\partial^2 T}{\partial y^2}\right), \tag{4}$$

where quantities are non-dimensionlized as follows:

$$t=\frac{t^*\kappa Ra^{1/2}}{H^2},\quad x=\frac{x^*}{H},\quad y=\frac{y^*}{H},\quad u=\frac{u^*H}{\kappa Ra^{1/2}},$$
$$v=\frac{v^*H}{\kappa Ra^{1/2}},\quad p=\frac{p^*H^2}{\rho\kappa^2 Ra},\quad T=\frac{T^*-T_0}{T_h-T_c}. \tag{5}$$

Here, the three dimensionless parameters which govern the flow are the Rayleigh number (Ra), the Prandtl number (Pr) and the aspect ratio (A), defined as

$$Ra=\frac{g\beta(T_h-T_c)H^3}{v\kappa}, \tag{6}$$

$$Pr=\frac{v}{\kappa}, \tag{7}$$

$$A=\frac{H}{L}. \tag{8}$$

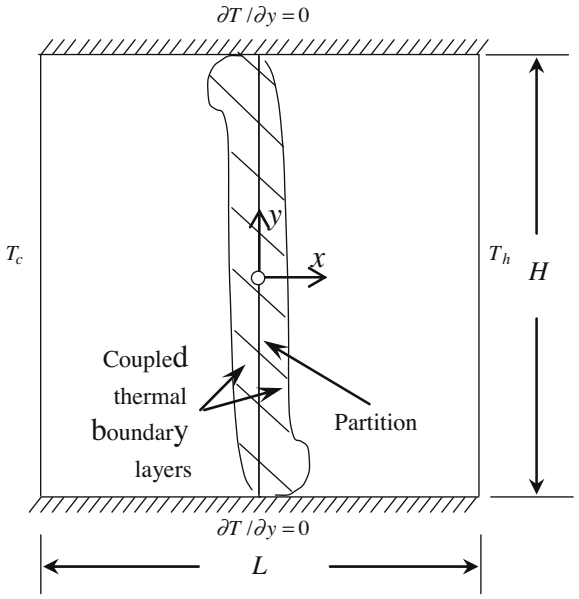

Fig. 1. Schematic of the physical problem.

Note that in this study the working fluid is water with a constant Prandtl number of $Pr = 6.63$; the aspect ratio of the overall cavity is unity ($A = 1$); and the Rayleigh number for the partitioned cavity is fixed at 9.2×10^8, which is of the same order as the Rayleigh number considered for a non-partitioned square cavity in [27], in which numerical results have been validated by corresponding experimental data. Furthermore, a Rayleigh number (Ra_T) based on the initial temperature difference across the thermal boundary layer (between the interior fluid and the partition or sidewall) is also adopted in this paper, and is defined as follows:

$$Ra_T = \frac{g\beta(T_P - T_i)H^3}{\nu\kappa}, \tag{9}$$

where T_P and T_i are the initial temperatures of the partition (or sidewall) and the interior fluid, respectively.

As shown in Fig. 1, the top and bottom walls of the cavity are adiabatic; the two sidewalls are isothermal and fixed at T_c (= −0.5) and T_h (= 0.5) respectively; the partition of a zero thickness is vertically placed in the centre of the cavity and is diathermal (for which only horizontal heat transfer is considered, refer to [24,25]); and all interior walls and the partition are rigid and no-slip. Accordingly, the boundary conditions are summarized as follows:

$$\begin{aligned} &u = v = 0, \quad T = 0.5 \quad \text{at } x = 0.5, \\ &u = v = 0, \quad T = -0.5 \quad \text{at } x = -0.5, \\ &u = v = 0, \quad \frac{\partial T}{\partial y} = 0 \quad \text{at } y = -0.5 \text{ and } 0.5 \end{aligned} \tag{10}$$

The working fluid is initially quiescent ($u = v = 0$). At $t = 0$, the temperature of the fluid on the left side of the partition is −0.5, and that on the right side of the partition is 0.5.

The governing equations are implicitly solved using a finite-volume SIMPLE algorithm. The advection terms are discretized by a QUICK scheme, and the time integration is by a second-order backward difference method (also see [27,28]).

Two non-uniform grid systems (423×298 and 541×538) with coarser grids in the core and finer grids concentrated in the proximity of all wall and partition boundaries were constructed for grid dependence tests. Fig. 2 plots time series of the temperatures at a point in the downstream end of the thermal boundary layer on the left side of the partition calculated using the two grid systems. Clearly, only very small variations may be observed at the occurrence of the second group of waves between the two sets of the numerical results. This means that either grid system is able to resolve the transient natural convection in the partitioned cavity and characterize the details of the boundary layers adjacent to the partition and sidewalls at the present Rayleigh number. In consideration of the computing time, the grid system of 423×298 with grid inflation factors (which are the ratio of two consecutive grid spacings along a given grid direction) of 1.0591 in the x-direction and 1.0135 in the y-direction is adopted in this study.

Two dimensionless time steps of 0.0075 and 0.0038 (much smaller than 0.0525 adopted by Patterson and Armfield [27]) are tested to examine the effect of the time step. The numerical results obtained using the two time steps are also plotted in Fig. 2. Evidently, the development of the flow is not sensitive to the two tested time steps, with either choice being satisfactory. Accordingly, the larger time step of 0.0075 is considered to be sufficiently small to capture the transient features of the flow development and is adopted here.

3. Transient flow development

The temperature time series in Fig. 2 illustrate the overall development of natural convection from a suddenly generated temperature difference between the fluids on the two sides of the partition to a steady state. The overall development may be roughly classified into three main stages: an initial stage, a transitional stage and a steady stage, as marked in Fig. 2. At the initial stage (from start-up to the time t_s), the temperature in the thermal boundary layer adjacent to the partition follows the one dimensional growth (with only x-dependence) predicted by, for example, Goldstein and Briggs [29]. Here t_s is the time at which the convection term balances the conduction term in the energy equation (4). The scaling relation describing t_s has been given by Patterson and Imberger [8] as

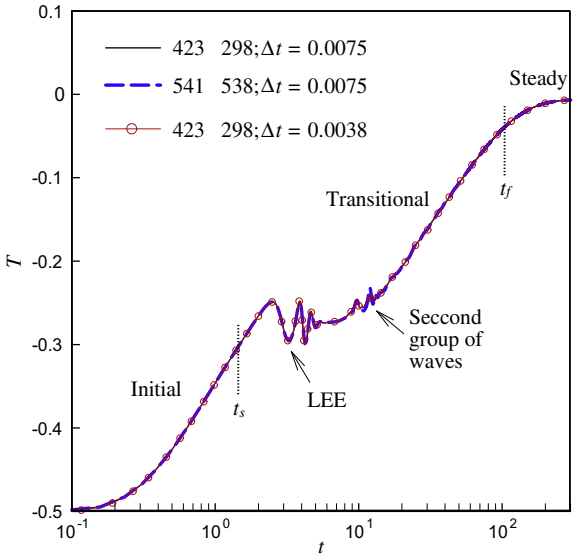

Fig. 2. Time series of the temperatures at the point ($x = -0.0083$, $y = 0.375$) in the downstream thermal boundary layer on the left side of the partition calculated using different meshes and time steps.

$$t_S \sim \frac{H^2}{\kappa Ra_T^{1/2}}. \tag{11}$$

Here, the initial temperature of the partition is T_0, and the temperature difference between the partition and the fluid at either side of the partition is $\Delta T/2$. Accordingly, the Rayleigh number Ra_T in (11) is calculated based on a temperature difference of $\Delta T/2$ for the present flow configuration.

As time increases, the development of the flow in the partitioned cavity enters into a transitional stage. As seen in Fig. 2, the temperature growth does not cease immediately after t_s. Instead, an overshoot of the temperature and subsequent travelling waves, which are characteristics of the leading edge effect (LEE, see [16–20]), are clearly present. A second group of waves may also be induced by internal gravity waves (see Section 3.2).

Associated with the formation of the coupled thermal boundary layers on the two sides of the partition, the thermal flows from the boundary layers are continuously discharged into the left and right cores of the partitioned cavity until the time t_f, where t_f is the time for the cavity to be filled up with the thermal fluid discharged from the coupled thermal boundary layers. Since the volumetric flow rate of the thermal boundary layer is $Q \sim k(Ra_T)^{1/4}$ [8], t_f may be estimated as

$$t_f \sim \frac{H\frac{L}{2}}{\kappa Ra_T^{1/4}} \sim \frac{Ra_T^{1/4}}{2A} t_s. \tag{12}$$

Note that here Ra_T, the same as that in (11), is also calculated based on a temperature difference of $\Delta T/2$.

For $t > t_f$, the rate of temperature growth with time decreases and the temperature at a particular location eventually approaches a constant value, as seen in Fig. 2. The development of natural convection then enters into a steady stage.

In the following sections, the transient features of the natural convection flow including the developments of the coupled thermal boundary layers, intrusions and internal gravity waves will be characterized. Furthermore, for the purpose of comparing between the thermal boundary layers adjacent to the partition and a suddenly heated isothermal sidewall and examining the effect of the partition on heat transfer, another two cases are also presented. One case is a square cavity (with $A = 1$) without a partition in which the boundary conditions on the top, bottom and sidewalls are identical to those for the partitioned case; and the other is a narrow cavity (with $A = 2$) which effectively constitutes the left half of the partitioned cavity with the partition and the fluid on the right half of the cavity replaced by an isothermal wall at the initial temperature of the fluid on the right half of the cavity. In the latter case, all other boundary conditions and the initial condition are the same as those of the left half of the partitioned cavity. The impact of the partition on the flow and heat transfer in a cavity may be quantified by comparing the partitioned and non-partitioned square cavity cases. Moreover, the variation of heat transfer through a thermal boundary layer adjacent to an isothermal vertical wall (a typical idealised scenario assumed in the literature, see for example [1]) and that through the coupled thermal boundary layers adjacent to a vertical wall (the realistic condition) may be examined through the comparison between the narrow cavity and the partitioned square cavity cases. The initial and boundary temperature conditions for all the three cases considered in this study are listed in Table 1 (here, the x- and y-velocities at the initial time and on all boundaries for all three cases are zero, i.e. $u = v = 0$). It is worth noting that the fluid on the left hand side of the partition is heated by the partition, whereas the fluid on the right side is cooled by the partition.

3.1. Coupled thermal boundary layers

Fig. 3(a) shows the time evolution of two isotherms ($T = -0.49$ and 0.49) on both sides of the partition following the sudden start-up. Clearly, in addition to the temperature growth close to the partition in the initial stage (seen in Fig. 2), the horizontal shift of the isotherms shows that the thickness of the coupled thermal boundary layers also increases with time. Note that the isotherms at the upstream end of the coupled thermal boundary layers show the presence of waves. This is a result of the LEE as the boundary layers undergo a transition from a one dimensional unsteady state to a two-dimensional steady state [18,20].

For the purpose of illustrating the scaling relation describing the thickness of the thermal boundary layers, the dependence of the calculated thickness on time is plotted in Fig. 3(b), where the thickness (δ_T) is defined as the distance between the isotherm of $T = -0.49$ and the partition at the mid height ($y = 0$). Furthermore, the calculated thicknesses of the thermal boundary layers adjacent to an isothermal sidewall for the non-partitioned square cavity and narrow cavity cases are also shown in Fig. 3(b). Patterson and Imberger [8] and others have pointed out that the thickness of the thermal boundary layer adjacent to an isothermal wall grows with time according to the scaling relation $\delta_T \sim k^{1/2}t^{1/2}$, which may also be expressed in a dimensionless form as $\delta_T Ra_T^{1/4} \sim t^{1/2}$. Fig. 3(b) shows a very good linear correlation between $\delta_T Ra_T^{1/4}$ and $t^{1/2}$ for all the three cases considered here, confirming that the scaling relation for the thickness of the thermal boundary layer adjacent to an isothermal wall also holds for the coupled thermal boundary layers. It is worth noting that for the narrow cavity case, Ra_T is double that of the other two cases since the initial temperature difference between the fluid and the hot sidewall is ΔT for the narrow cavity case (see Table 1).

To illustrate further transient features of the coupled thermal boundary layers, Fig. 4 shows comparisons between the time series of the temperatures at the specified point in the downstream thermal boundary layers for all the three cases. Note that for the purpose of comparing different thermal boundary layers for all the three cases, the normalized temperature growths in the thermal boundary layers with reference to the initial interior fluid temperatures are plotted in this figure. Clearly, the temperature growth in the thermal boundary layer adjacent to the partition is consistent with that adjacent to the isothermal sidewall for the non-partitioned square cavity case except for some variations during the occurrence of travelling waves. This is because the initial temperature difference between the partition and the fluid is the same as that between the sidewall and the fluid for the non-partitioned square cavity case ($= \Delta T/2$, see Table 1); and in the initial stage, the partition is approximately isothermal (which is also confirmed by the following numerical results). However, for the narrow cavity case, the initial temperature difference between the sidewall and the interior fluid is ΔT (doubling that for the partitioned cavity case, see Table 1), which results in a faster temperature growth different from that adjacent to the partition, as seen in Fig. 4.

Fig. 5 shows the development of the temperature structure within the coupled thermal boundary layers. It is seen from Fig. 5(a) that the vertical temperature profiles on the partition ($x = 0$) change from an initially isothermal to an approximately linear vertical distribution between $y = -0.4$ and $y = 0.4$ at the steady stage (e.g. $t = 300$). Since in the initial stage there is a temperature difference between the partition and the fluid on the left side of the partition similar to that between the isothermal sidewall and the fluid for the non-partitioned square cavity case, the temperature growth in the thermal boundary layer adjacent to the partition in the initial stage is also similar to that adjacent to the sidewall in the non-partitioned square cavity case (refer to Fig. 4). Furthermore, Fig. 5(b) shows the evolution of the horizontal temperature profiles of the coupled thermal boundary layers. Clearly, the temperature of the interior fluid on the left side of the partition is approximately -0.5 and that on the right side of the partition is 0.5 at the early stage (e.g. $t = 0.5$, 1 and 6, also see the zoomed plot for details). However, as the thermal fluid is continuously discharged from the coupled thermal boundary layers into the cavity, the temperature of the interior fluid on the left at $y = 0$ apparently increases and that on the right decreases, particularly for $t \geqslant t_f/2$ ($= 52$ for the present Rayleigh number).

Table 1
Initial and boundary temperature conditions for all the three cases.

	Initial fluid temperature	Temperatures on wall boundaries		
		Cold sidewall	Hot sidewall	Top and bottom
Partitioned square cavity	$T = -0.5$ on the left of the partition; $T = 0.5$ on the right of the partition ($T = 0$ on the partition)	$T = -0.5$	$T = 0.5$	$\partial T/\partial y = 0$
Square cavity ($A = 1$)	$T = 0$	$T = -0.5$	$T = 0.5$	$\partial T/\partial y = 0$
Narrow cavity ($A = 2$)	$T = -0.5$	$T = -0.5$	$T = 0.5$	$\partial T/\partial y = 0$

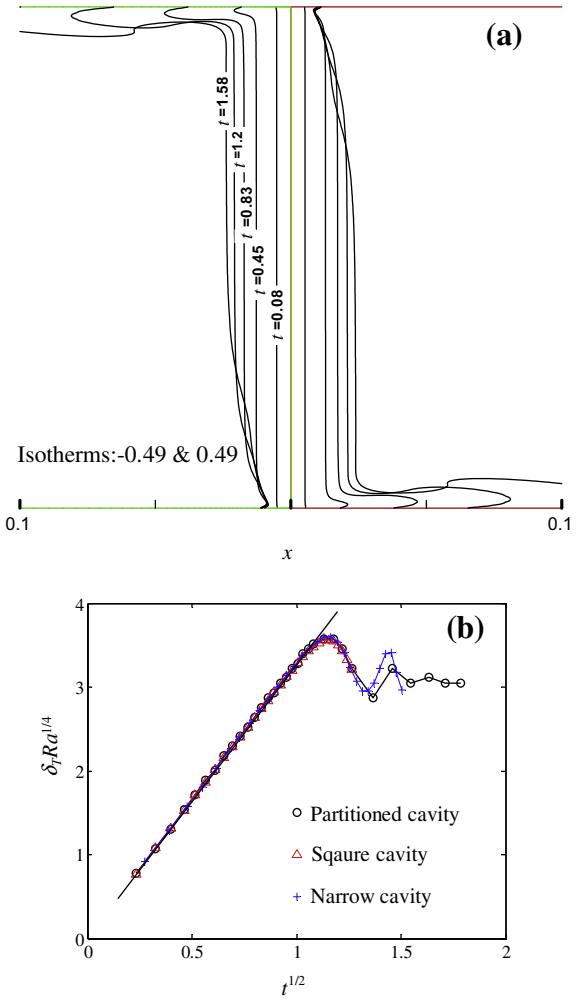

Fig. 3. Growth of the thermal boundary layers. (a) Isotherms at different times. (b) Time series of the thickness of the thermal boundary layers at $y = 0$ for all the three cases.

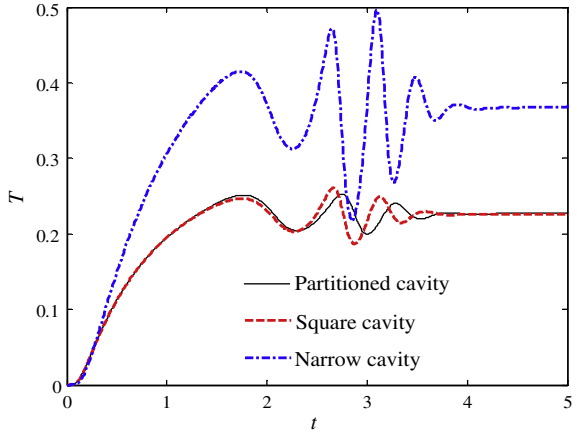

Fig. 4. Time series of the temperatures obtained at a point 0.0083 away from the partition for the partitioned square cavity case or the sidewall for the non-partitioned square cavity and narrow cavity cases and 0.875 away from the leading edge of the partition or sidewall.

3.2. Intrusions and internal gravity waves

Previous studies (e.g. [8]) have shown that a horizontal wall of a differentially heated cavity forces an intrusion to be discharged from the vertical thermal boundary layer into the core. Fig. 6(a) and (b) shows the temperature and flow structures of the intrusion, which are similar to the experimental observations in a non-partitioned cavity with a comparable Rayleigh number (based on the temperature difference across the thermal boundary layer) reported in Patterson and Armfield [27] and Xu et al. [30]. Note that since the laminar natural convection in the partitioned cavity for the present Rayleigh number is centro-symmetric about the origin (which is illustrated by the time series of the temperatures at two centro-symmetric points in Fig. 6(c) but is not further exploited in the numerical solution, refer to [25]), the isotherms and streamlines are shown in one half of the cavity only in Fig. 6(a) and (b), respectively.

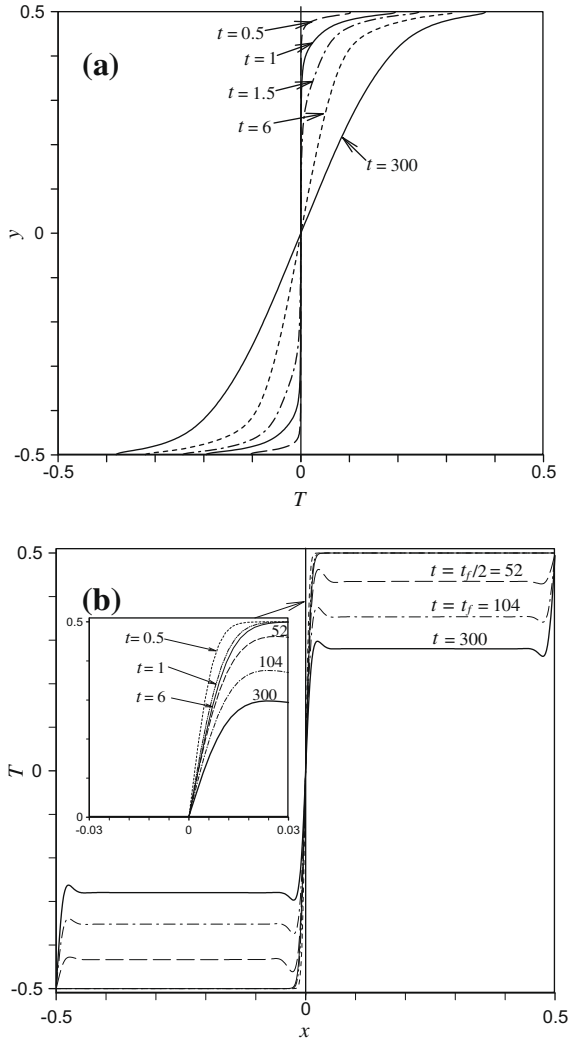

Fig. 5. Temperature profiles in the coupled thermal boundary layers at different times. (a) Vertical profiles on the partition ($x = 0$). (b) Horizontal profiles at $y = 0$ (here t_f is specified by (10)).

As time increases, the intrusions strike the isothermal sidewalls. Fig. 7(a) shows an inclined isotherm in the core on the left side of the partition. As pointed out by Patterson and Imberger [8], such an inclined isotherm may induce internal gravity waves in the cavity; that is, the tilting isotherm is oscillatory, as shown in Fig. 7(b) and (c). For the purpose of illustrating the presence of internal gravity waves, a time series of the x-velocity (u) at a point close to the top wall is plotted in Fig. 7(d), in which the times corresponding to Fig. 7(a)–(c) are marked. Clearly, internal gravity waves are present (e.g. for $t < 40$) but are significantly damped out after $t = 100$.

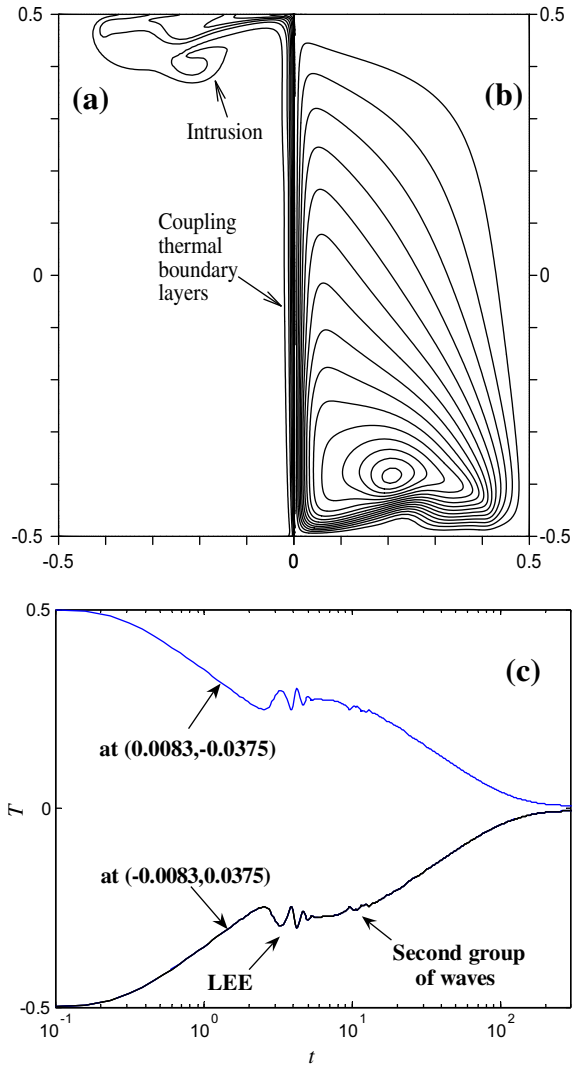

Fig. 6. Intrusion in the partitioned cavity. (a) Isotherms on the left side of the partition: from −0.4375 to 0.4375 with an interval of 0.0975 at $t = 3.7636$. (b) Streamlines on the right side of the partition: from 0.0012 to 0.0173 with an interval of 0.0012 at $t = 3.7636$. (c) Time series of the temperatures at two centro-symmetric points.

Indeed, these strong internal gravity waves may trigger a convective instability on the coupled thermal boundary layers, which are indicated by the second group of travelling waves, as seen in Figs. 2 and 6(c).

To examine the effect of the partition on horizontal convection flows, volumetric flow rates, defined below (see [31]),

$$Q = \frac{1}{2}\int_{-1/2}^{1/2} |u|\, dy, \tag{13}$$

are calculated across the vertical plane at $x = -0.25$ for all three cases and plotted in Fig. 8. Note that the oscillations of the volumetric flow rate in the early stage are the result of internal gravity waves. Furthermore, it is seen from this figure that due to the blocking effect of the partition, the volumetric flow rate in the partitioned cavity is smaller (approximately 37% lower) than those in the non-partitioned square and narrow cavity cases in the steady stage (e.g. at $t = 300$). Clearly, the horizontal convection is depressed due to the presence of the partition.

It can be seen in Fig. 7(a)–(c) that a given isotherm gradually moves downwards as the thermal flow discharged from the coupled thermal boundary layers fills up the cavity. Ultimately, the fluid in the cavity becomes stratified. Fig. 9(a) shows the development of the stratification in the core at $x = -0.25$. It is clear that the temperature structure is initially uniform in the core (see e.g. $t = 6$) and approaches an approximately linear distribution (e.g. at $t = 300$) except in the proximity of the top and bottom walls. Fig. 9(b) shows the time evolution of the stratification parameter ($S = \partial T/\partial y$) in all cases. The stratification parameter at $t = 300$ is smaller than that for the non-partitioned square cavity case except for that in the proximity of the top wall; that is, due to the presence of the partition, the overall stratification in the cavity becomes weaker than that for the non-partitioned square cavity case.

Fig. 10 shows the temperature structure on the left side of the partition and the flow structure on the right side of the partition at the steady stage. It is seen in Fig. 10(a) that a thermal boundary layer adjacent to the far-left isothermal sidewall is ultimately formed (also see [28]). It is worth noting that, as illustrated by the streamlines in Fig. 10(b), the thermal boundary layers adjacent to the partition and sidewall are not symmetric with respect to the centre of each half of the cavity. This is because the boundary conditions of the thermal boundary layers adjacent to the partition and sidewall are different at the steady state; that is, the sidewall is isothermal but the temperature on the partition varies with the height (refer to Fig. 5(a)). It will become clear that the partition is approximately isoflux at the steady state, which is confirmed by the following numerical results.

4. Heat transfer

Previous studies (e.g. [24]) show that, for a laminar flow regime, a vertical partition in a differentially heated cavity apparently depresses heat transfer through the cavity. In this section, the effect of the partition on transient heat transfer will be examined. For the purpose of illustrating quantitatively the effect of the partition, both local and overall Nusselt numbers (Nu_y and Nu) are calculated on a rigid heat transfer surface (either the partition or a sidewall). By definition, the Nusselt number represents the ratio of convective heat transfer rate over conductive heat transfer rate. For the present investigation, heat is ultimately transferred from one sidewall to the other, and thus the separation between the two sidewalls (with or without the partition) is an appropriate length scale for calculating the conductive heat transfer rate. This results in the following definitions for the local and overall Nusselt numbers in non-dimensional form:

$$Nu_y = \frac{1}{A}\frac{\partial T}{\partial x}, \quad Nu = \frac{1}{A}\int_{-1/2}^{1/2} \frac{\partial T}{\partial x}\, dy. \tag{14}$$

For the purpose of quantifying the effect of the partition on heat transfer through the square cavity, Fig. 11(a) shows the time series of the overall Nusselt numbers calculated on the partition and sidewall for the partitioned and non-partitioned square cavity cases. For the partitioned case, due to the zero temperature difference between the fluid and isothermal sidewall at the initial stage, the calculated overall Nusselt number on the isothermal sidewall is negligibly small until $t = 5$. After the intrusion from the coupled thermal boundary layer strikes the isothermal sidewall, the overall Nusselt number on the isothermal sidewall starts to increase. Eventually it approaches the same value as the overall Nusselt number calculated on the partition, as expected from energy conservation.

Since the temperature distribution on the partition in the initial stage (except for that close to the two ends, see Fig. 5(a)) is approximately isothermal and the initial temperature difference between the partition and the interior fluid is the same as that for the non-partitioned square cavity case, there is a good agreement between the temperature structures in the thermal boundary layer adjacent

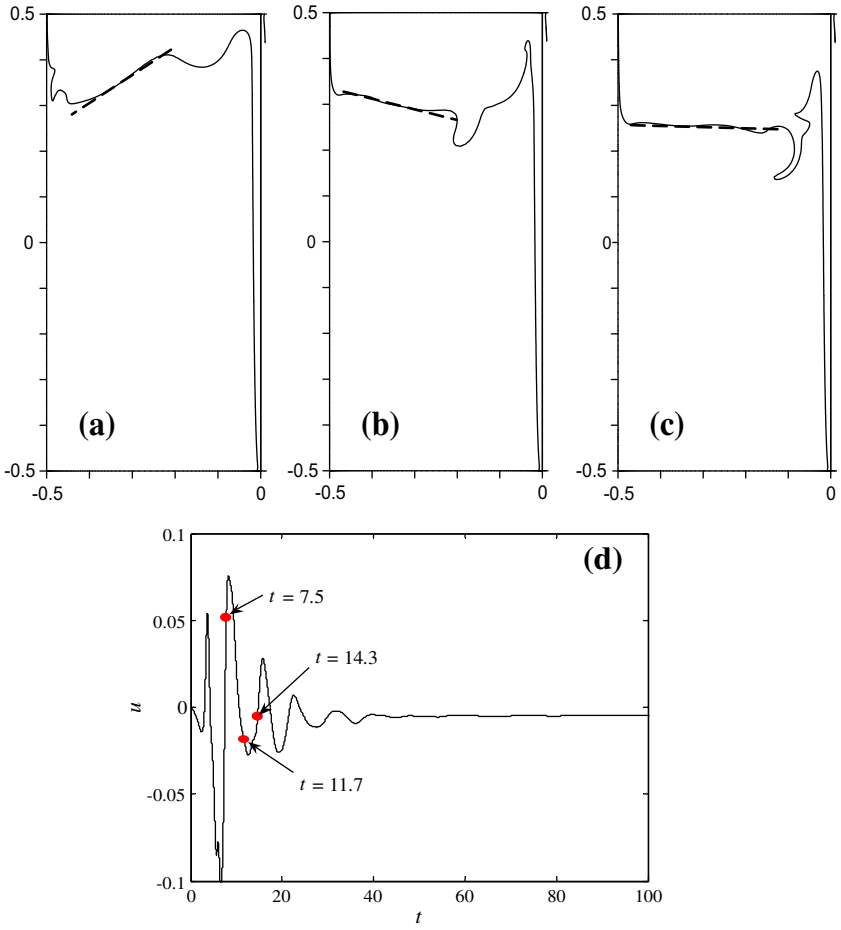

Fig. 7. Internal gravity waves induced by the intrusion in the partitioned cavity. (a), (b) and (c): The −0.4375 isotherm on the left side of the partition at $t = 7.5$, 11.7 and 14.3, respectively (the thick dashed line is used to illustrate oscillations of the tilting isotherm). (d) Time series of the x-velocity (u) at the point ($x = -0.3333$, $y = 0.375$) close to the tope wall on the left side of the partition.

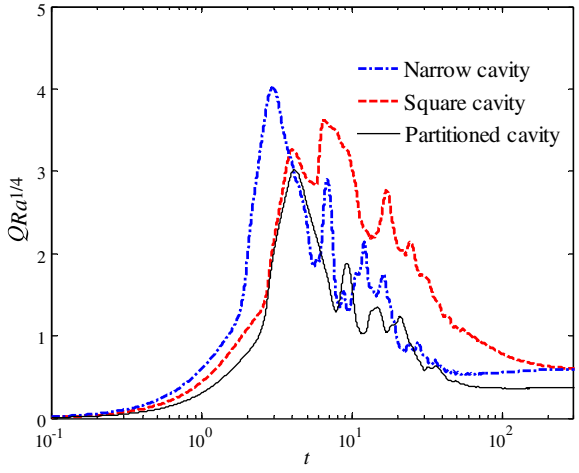

Fig. 8. Time series of the volumetric flow rates at $x = -0.25$ for all the three cases.

to the isothermal sidewall for the non-partitioned square cavity case and in the coupled thermal boundary layers adjacent to the partition in the initial stage, as seen in Fig. 4. As a consequence, the calculated overall Nusselt number on the isothermal sidewall of the non-partitioned square cavity is in general consistent with that on the partition for $t < 1$ (see Fig. 11). However, as shown in Fig. 5(a), the approximately isothermal condition on the partition lasts only for a short while after the start-up, and the temperatures near the two ends of the partition deviate from zero. This temperature distribution on the partition may have resulted in the slightly higher heat transfer through the partition than that through the isothermal sidewall for the non-partitioned case until $t = 9$.

For the non-partitioned square cavity case at $t > 9$, since the cold intrusion coming from the cold sidewall strikes the hot sidewall, the temperature difference between the hot sidewall and the fluid entrained from the cold intrusion to the thermal boundary layer is much larger than that between the partition and the fluid entrained into the coupled thermal boundary layers. As a consequence, the calculated overall Nusselt number on the hot sidewall for the non-partitioned square cavity case surpasses that on the partition, as seen in Fig. 11(a). At the steady state, $NuRa^{-1/4}$ on the sidewall for the non-partitioned square cavity case is 0.32, which is double that on the partition ($NuRa^{-1/4} = 0.16$). This result is consistent with that reported by Nishimura et al. [26].

In order to compare heat transfer through the coupled thermal boundary layers (on the two sides of the partition) with that through the thermal boundary layer adjacent an isothermal wall, Fig. 11(b) shows the time series of the overall Nusselt numbers calculated on the partition and the sidewall of the narrow cavity. In the literature, the latter case is often used to simulate the former case (realistic situations); that is, the thermal boundary layer on the other side of a vertical wall (the partition in the present case) is ignored, as noted in the introduction (also see [1]). Since the left half of the partitioned cavity is compared with the narrow cavity here, the aspect ratio (A) in (12) is 2 for both cases in Fig. 11(b), and thus the calculated $NuRa^{-1/4}$ on the partition is half of that pre-

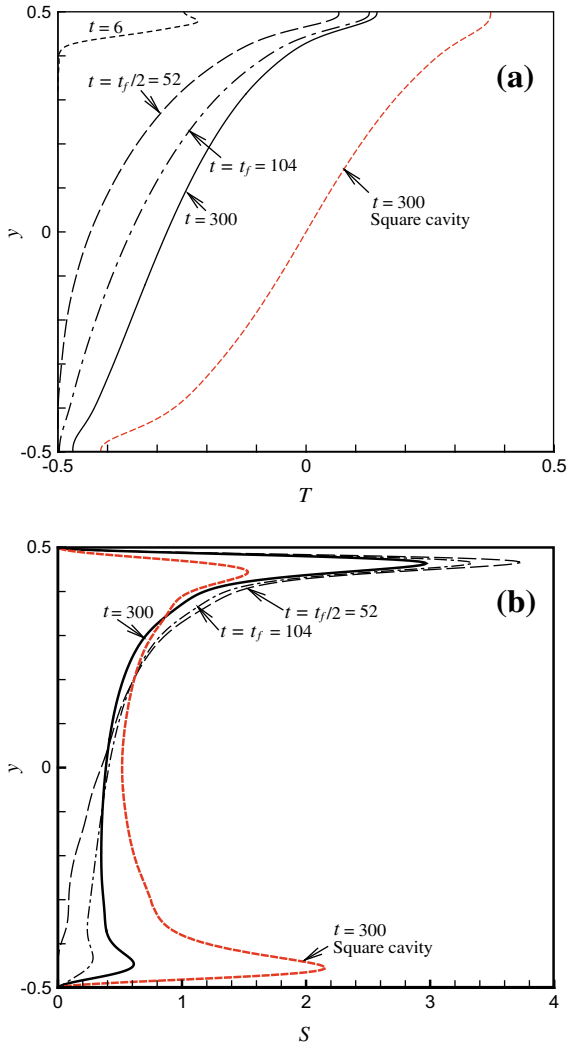

Fig. 9. Vertical profiles of the temperatures and stratification parameters (S) at $x = -0.25$ at different times for the partitioned and non-partitioned square cavity cases. (a) Temperature profiles. (b) Stratification parameter profiles.

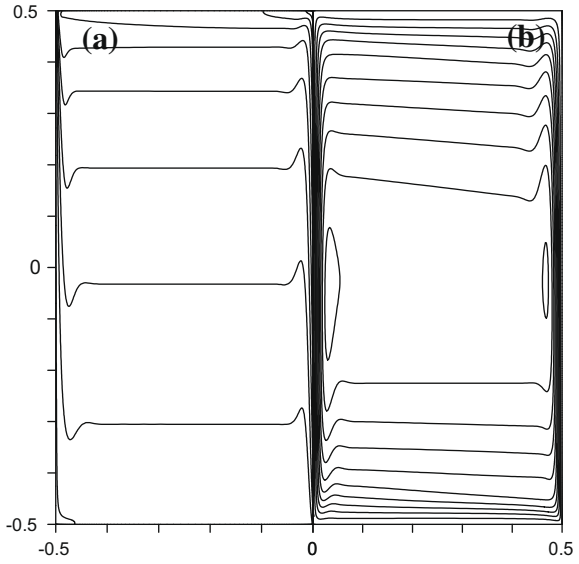

Fig. 10. Temperature and flow structures of natural convection at steady state ($t = 300$). (a) Isotherms on the left side of the partition from −0.4375 to 0.4375 with an interval of 0.0975. (b) Streamlines on the right side of the partition from 0.0014 to 0.0219 with an interval of 0.0023.

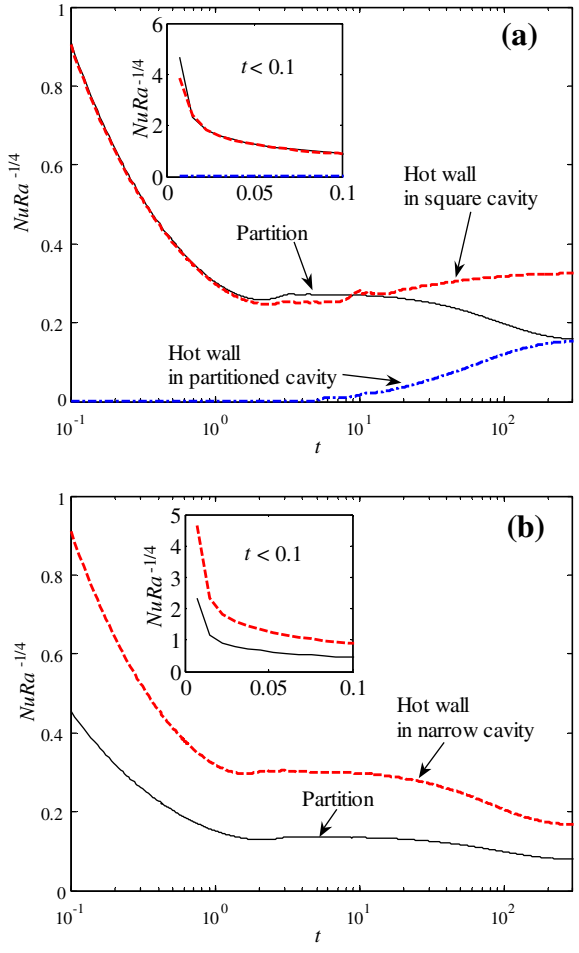

Fig. 11. Time series of the overall Nusselt numbers calculated on the partition and sidewall for all the three cases.

sented in Fig. 11(a). Clearly, the calculated overall Nusselt number on the hot sidewall of the narrow cavity is basically double that on the partition throughout the development of the natural convection flows, as seen in Fig. 11(b) (also see the zoomed plot for the very early stage of the flow development). This is because in the initial stage, the temperature difference between the sidewall and the interior fluid for the narrow cavity case is ΔT, double that between the partition and the interior fluid on the left side of the partition (see Table 1). As a result, the heat transfer rate through the sidewall of the narrow cavity is approximately double that on the partition. Furthermore, in the steady stage, heat transfer through the sidewall of the narrow cavity is also approximately double that on the partition since the temperature difference between two sidewalls of the narrow cavity is double the average temperature difference ($\Delta T/2$) between the left sidewall and the partition of the partitioned square cavity. The result shown in Fig. 11(b) indicates that neglecting the presence of the coupled thermal boundary layers in real situations and representing it with a single thermal boundary layer adjacent to an isothermal wall results in a significant over-estimation of heat transfer through the wall.

Fig. 12 shows the vertical profiles of the local Nusselt numbers (here $A = 1$ in the calculation of the local Nusselt number) at the steady state on the partition and hot sidewall for the partitioned square cavity case. It is clear that the local Nusselt number on the sidewall is non-uniform, and the local Nusselt number in the

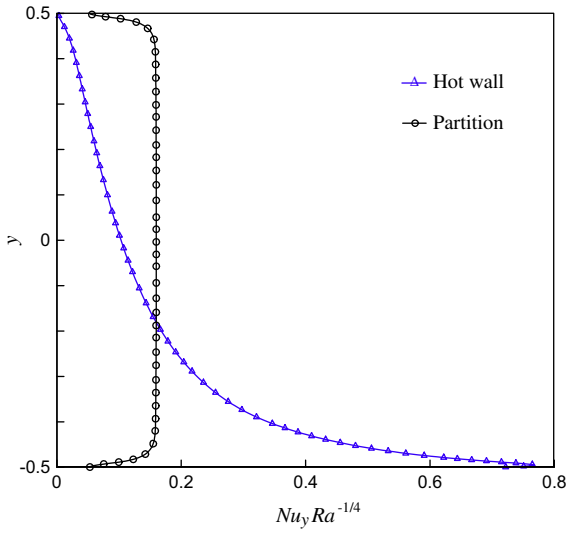

Fig. 12. Profiles of the local Nusselt numbers on the partition and sidewall for the partitioned square cavity case.

upstream section of the hot sidewall is much larger than that in the downstream section of the hot sidewall due to the stratification in the core. However, the local Nusselt number on the partition is approximately constant over the full height except for the two ends; that is, the heat transfer rate through the partition does not vary with the height except for in the proximity to the top and bottom walls. This implies that the partition is approximately isoflux at the steady state. Therefore, an interesting flow condition is reached at the steady state with the two thermal boundary layers governed by different thermal forcing: one is the coupled thermal boundary layers adjacent to the partition subject to an approximately isoflux boundary condition, and the other is the thermal boundary layer adjacent to the sidewall subject to isothermal thermal forcing (the flow is not symmetric with respect to the centre of either half of the cavity).

5. Conclusions

In this paper, the coupled thermal boundary layers induced by a suddenly generated temperature difference between the fluids on the two sides of a partition in a differentially heated cavity are investigated numerically. The transient features of natural convection flows in the partitioned cavity are characterized, and the development of natural convection flows has been classified into three distinct stages: an initial stage, a transitional stage and a steady stage. The time scales quantifying the three stages are estimated.

In the initial stage, coupled thermal boundary layers are formed on both sides of the partition, and the leading edge effect (LEE), which is present on both sides of the partition and plays a key role in the transition of the thermal boundary layer to a steady state, is observed. The dependence of the thermal boundary layer thickness on time is found to be consistent with the scaling relation given by Patterson and Imberger [8]. In the transition to the steady state, as the thermal flows discharged from the downstream ends of the coupled thermal boundary layers continuously fill each half of the partitioned cavity, additional thermal boundary layers form adjacent to the isothermal sidewalls. A phenomenon of particular interest in the transient flow development is that the temperature distribution on the partition enclosed by the coupled thermal boundary layers changes from an initially isothermal to an approximately linear profile at the steady state. As a consequence, an approximately isoflux condition is established across the partition in the steady state. Clearly, the usual assumption of an isothermal wall in this configuration is incorrect.

Apart from the variations in the temperature distributions between an isothermal vertical wall and a vertical wall between the coupled thermal boundary layers (i.e. the partition), heat transfer through the coupled thermal boundary layers is considerably lower than that through the corresponding thermal boundary layer adjacent to an isothermal wall. Therefore, neglecting the effect of coupled thermal boundary layers, which is present in many real life situations, will cause an over-estimation of heat transfer through a wall. For the present Rayleigh number, heat transfer through the coupled thermal boundary layers is only half of that through the corresponding thermal boundary layer adjacent to an isothermal wall.

The evolution of the intrusions and the stratification in the cores on both sides of the partition show features similar to those in a non-partitioned cavity. However, the quantitative comparisons presented in this study have shown variations between the partitioned and non-partitioned square cavity cases. Due to the presence of the partition, the stratification in the core becomes weaker and the horizontal convective flows are significantly depressed. For the present Rayleigh number, the volumetric flow rate is depressed by approximately 37% and heat transfer depressed by 50% by the single partition.

Acknowledgment

This research was funded by the Australian Research Council.

References

[1] J.M.F. Oro, C.S. Morros, K.M.A. Diaz, P.L.G. Ybarra, Numerical simulation of the fuel oil cooling process in a wrecked ship, J. Fluids Eng. 128 (2006) 1390–1393.
[2] G.K. Bachelor, Heat transfer by free convection across a closed cavity between vertical boundaries at different temperatures, Quart. Appl. Math. 12 (1954) 209–233.
[3] E.R.G. Eckert, W.O. Carlson, Natural convection in an air layer enclosed between two vertical plates at different temperatures, Int. J. Heat Mass Transfer 2 (1961) 106–129.
[4] J.W. Elder, Laminar free convection in a vertical slot, J. Fluid Mech. 23 (1965) 77–98.
[5] A.E. Gill, The boundary-layer regime for convection in a rectangular cavity, J. Fluid Mech. 26 (1966) 515–536.
[6] G. De Vahl Davis, Natural convection of air in a square cavity: a bench mark numerical solution, Int. J. Numer. Methods Fluids 3 (1983) 249–264.
[7] A.E. Gill, A. Davey, Instabilities of a buoyancy-driven system, J. Fluid Mech. 35 (1969) 775–798.
[8] J.C. Patterson, J. Imberger, Unsteady natural convection in a rectangular cavity, J. Fluid Mech. 100 (1980) 65–86.
[9] D.R. Chenoweth, S. Paolucci, Natural convection in an enclosed vertical air layer with large horizontal temperature differences, J. Fluid Mech. 169 (1986) 173–210.
[10] S. Paolucci, D.R. Chenoweth, Transition to chaos in a differentially heated vertical cavity, J. Fluid Mech. 201 (1989) 379–410.
[11] P. Le Quere, Transition to unsteady natural convection in a tall water-filled cavity, Phys. Fluids 2 (1990) 503–515.
[12] P. Le Quere, M. Behnia, From onset of unsteadiness to chaos in a deferentially heated square cavity, J. Fluid Mech. 359 (1998) 81–107.
[13] J.W. Elder, Turbulent free convection in a vertical slot, J. Fluid Mech. 23 (1965) 99–111.
[14] S. Paolucci, Direct numerical simulation of two-dimensional turbulent natural convection in an enclosed cavity, J. Fluid Mech. 215 (1990) 229–262.
[15] H.S. Dol, K. Hanjalic, Computational study of turbulent natural convection in a side-heated near-cubic enclosure at a high Rayleigh number, Int. J. Heat Mass Transfer 44 (2001) 2323–2344.
[16] S.G. Schladow, Oscillatory motion in a side-heated cavity, J. Fluid Mech. 213 (1990) 589–610.
[17] S.G. Schladow, J.C. Patterson, R.L. Street, Transient flow in a side-heated cavity at high Rayleigh number: a numerical study, J. Fluid Mech. 200 (1989) 121–148.
[18] S.W. Armfield, J.C. Patterson, Wave properties of natural-convection boundary layers, J. Fluid Mech. 239 (1992) 195–211.

[19] W. Schöpf, J.C. Patterson, Natural convection in a side-heated cavity: visualization of the initial flow features, J. Fluid Mech. 295 (1995) 357–379.
[20] J.C. Patterson, T. Graham, W. Schöpf, S.W. Armfield, Boundary layer development on a semi-infinite suddenly heated vertical plate, J. Fluid Mech. 453 (2002) 39–55.
[21] T. Nishimura, M. Shiraishi, Y. Kawamura, Natural convection heat transfer in enclosures with an off-center partition, Int. J. Heat Mass Transfer 30 (1987) 1756–1758.
[22] D. Duxbury, An interferometric study of natural convection in enclosed plane air layers with complete and partial central vertical divisions, Ph.D. Thesis, University of Salford, 1979.
[23] D.M. Cuckovic-Dzodzo, M.B. Dzodzo, M.D. Pavlovic, Laminar natural convection in a fully partitioned enclosure containing fluid with nonlinear thermopysical properties, Int. J. Heat Fluid Flow 20 (1999) 614–623.
[24] R. Anderson, A. Bejan, Natural convection on both sides of a vertical wall separating fluids at different temperature, J. Heat Transfer 102 (1980) 630–635.
[25] R. Anderson, A. Bejan, Heat transfer through single and double vertical walls in natural convection: theory and experiment, Int. J. Heat Mass Transfer 24 (1981) 1611–1620.
[26] T. Nishimura, M. Shiraishi, F. Nagasawa, Y. Kawamura, Natural convection heat transfer in enclosures with multiple vertical partitions, Int. J. Heat Mass Transfer 31 (1988) 1679–1686.
[27] J.C. Patterson, S.W. Armfield, Transient features of natural convection in a cavity, J. Fluid Mech. 219 (1990) 469–497.
[28] F. Xu, J.C. Patterson, C. Lei, On the double-layer structure of the boundary layer adjacent to a sidewall of a differentially-heated cavity, Int. J. Heat Mass Transfer 51 (2008) 3803–3815.
[29] R.J. Goldstein, D.G. Briggs, Transient free convection about vertical plates and cylinders, J. Heat Transfer 86 (1964) 490–500.
[30] F. Xu, J.C. Patterson, C. Lei, Shadowgraph observations of the transition of the thermal boundary layer in a side-heated cavity, Exp. Fluids 38 (2005) 770–779.
[31] C. Lei, J.C. Patterson, Unsteady natural convection in a triangular enclosure induced by absorption of radiation, J. Fluid Mech. 460 (2002) 181–209.